From Weakly Coordinating to Non-Coordinating Anions? A Simple Preparation of the Silver Salt of the Least Coordinating Anion and Its Application To Determine the Ground State Structure of the $Ag(\eta^2\text{-}P_4)_2^+$ Cation

Angela Bihlmeier, Marcin Gonsior, Ines Raabe, Nils Trapp, and Ingo Krossing*[a]

Abstract: The unexpected but facile preparation of the silver salt of the *least* coordinating $[(RO)_3Al\text{-}F\text{-}Al(OR)_3]^-$ anion ($R=C(CF_3)_3$) by reaction of $Ag[Al(OR)_4]$ with one equivalent of PCl_3 is described. The mechanism of the formation of $Ag[(RO)_3Al\text{-}F\text{-}Al(OR)_3]$ is explained based on the available experimental data as well as on quantum chemical calculations with the inclusion of entropy and COSMO solvation enthalpies. The crystal structures of $(RO)_3Al{\leftarrow}OC_4H_8$, $Cs^+[(RO)_2(Me)Al\text{-}F\text{-}Al(Me)(OR)_2]^-$, $Ag(CH_2Cl_2)_3^+[(RO)_3Al\text{-}F\text{-}Al(OR)_3]^-$ and $Ag(\eta^2\text{-}P_4)_2^+[(RO)_3Al\text{-}F\text{-}Al(OR)_3]^-$ are described. From the collected data it will be shown that the $[(RO)_3Al\text{-}F\text{-}Al(OR)_3]^-$ anion is the *least* coordinating anion currently known. With respect to the fluoride ion affinity of two parent Lewis acids $Al(OR)_3$ of 685 kJ mol^{-1}, the ligand affinity (441 kJ mol^{-1}), the proton and copper decomposition reactions (−983 and −297 kJ mol^{-1}) as well as HOMO level and HOMO–LUMO gap and in comparison with $[Sb_4F_{21}]^-$, $[Sb(OTeF_5)_6]^-$, $[Al(OR)_4]^-$ as well as $[B(R^F)_4]^-$ ($R^F=CF_3$ or C_6F_5) the $[(RO)_3Al\text{-}F\text{-}Al(OR)_3]^-$ anion is among the best weakly coordinating anions (WCAs) according to each value. In contrast to most of the other cited anions, the $[(RO)_3Al\text{-}F\text{-}Al(OR)_3]$ anion is available by a simple preparation in conventional inorganic laboratories. The least coordinating character of this anion was employed to clarify the question of the ground state geometry of the $Ag(\eta^2\text{-}P_4)_2^+$ cation (D_{2h}, D_2 or D_{2d}?). In agreement with computational data and NMR spectra it could be shown that the rotation along the Ag-(P-P-centroid) vector has no barrier and that the structure adopted in the solid state depends on packing effects which lead to an almost D_{2h} symmetric $Ag(\eta^2\text{-}P_4)_2^+$ cation (0 to 10.6° torsion) for the more symmetrical $[Al(OR)_4]^-$ anion, but to a D_2 symmetric $Ag(\eta^2\text{-}P_4)_2^+$ cation with a 44° twist angle of the two AgP_2 planes for the less symmetrical $[(RO)_3Al\text{-}F\text{-}Al(OR)_3]^-$ anion. This implies that silver back bonding, suggested by quantum chemical population analyses to be of importance, is only weak.

Keywords: cations · density functional calculations · phosphorus · silver · weakly coordinating anion

Introduction

Chemistry with very *w*eakly *c*oordinating *a*nions (WCAs) is world wide an active area of research that is of great importance in applied as well as fundamental science.[1a–d,2] Applications of WCAs include for example olefin polymerization with cationic metallocene based catalysts,[1c] Li ion catalyzed En- or Diels–Alder reactions,[3] electrolytes for Li-ion batteries,[4] supporting electrolytes for electrochemistry[5] and new ionic liquids.[6] In more fundamental science chemically robust WCAs allow to stabilize unusual reactive or weakly bound cations such as $Au(Xe)_4^{2+}$,[7] Xe_2^+,[8] HC_{60}^+,[9] Mes_3Si^+,[10] $Ag(CO)_2^+$,[11] N_5^+,[12] $Ir(CO)_6^{3+}$,[13] $Ag(L)_x^+$ (L = P_4,[14] P_4S_3,[15] S_8,[16] C_2H_4[17]), $P_5X_2^+$ (X = Br, I)[18] or CI_3^+.[19] A few years ago we reported on WCAs of type $[Al(OR^F)_4]^-$ (R^F = poly- or perfluorinated aliphatic alkoxide).[20–22] The perfluorinated anion with $R=C(CF_3)_3$[20] emerged jointly with $[1\text{-}H\text{-}CB_{11}Me_5Cl_6]^-$,[23] $[1\text{-}Et\text{-}CB_{11}F_{11}]^-$,[24] $[CB_{11}(CF_3)_{12}]^-$,[25] $[Sb_4F_{21}]^-$,[26] $[Sb(OTeF_5)_6]^-$[27] and $[B(CF_3)_4]^-$[28] as one of the least coordinating anions currently known. Moreover it is chemically very robust, so

[a] A. Bihlmeier, M. Sc. M. Gonsior, Dipl.-Chem. I. Raabe, Dipl.-Chem. N. Trapp, Dr. I. Krossing
Universität Karlsruhe, Institut für Anorganische Chemie
Engesserstrasse, Geb. 30.45, 76128 Karlsruhe (Germany)
Fax: (+49) 721 608 48 54
E-mail: krossing@chemie.uni-karlsruhe.de

Supporting information for this article is available on the WWW under http://www.chemeurj.org/ or from the author: Additional structural parameters of the solid-state structures, drawings of solid state cation–anion contacts in **3**, the experimental $P_5Cl_2^+$ spectrum, *xyz* coordinates of the BP86/SV(P) optimized structures of $Al(OR)_3$, $Al(OR)_4^-$ and $(RO)_3Al\text{-}F\text{-}Al(OR)_3^-$ as well as calculated vibrational frequencies of $Ag(CH_2Cl_2)_3^+$ are deposited in the electronic Supporting Information (5 Tables, 2 Figures).

 DOI: 10.1002/chem.200400096

that a CD_2Cl_2 solution of the triiodocarbeniumion salt $CI_3^+[Al(OR)_4]^-$[19] is stable over days at RT.

However, we repeatedly observed that $[Al(OR)_4]^-$ dissolved in CH_2Cl_2 decomposed in the presence of very electrophilic cations such as $P_2X_5^+$ (X = Br, I) at temperatures above −20 °C to give the fluoride bridged $[(RO)_3Al\text{-}F\text{-}Al(OR)_3]^-$ anion.[18a,29] According to an analysis of the structural parameters, this anion is more stable than $[Al(OR)_4]^-$;[18] its negative charge is dispersed over a surface built from 54 peripheral C–F vs. 36 C–F bonds in $[Al(OR)_4]^-$. Thus one could argue that the fluoride bridged anion has a "Teflon-coating" which reduces its ability to act as a source of coordination. Therefore, the $[(RO)_3Al\text{-}F\text{-}Al(OR)_3]^-$ anion with the world record of 54 peripheral C–F bonds is the least coordinating anion currently known, which as such could also be addressed as almost non-coordinating. To date only $Cl_2P(CHCl_2)_2^+$, $P_2I_5^+$ and $P_3I_6^+$ salts of this anion are known.[18a,29] Herein we report on the straightforward but unexpected synthesis of the silver salt of the fluoride bridged $[(RO)_3Al\text{-}F\text{-}Al(OR)_3]^-$ anion that may be used in general chemistry to introduce this anion into a given system by metathesis reactions. Moreover we report on the first application of the least coordinating character of this anion to establish the ground state structure[14] of the $Ag(\eta^2\text{-}P_4)_2^+$ cation (D_{2h}, D_2 or D_{2d}?).

Results and Discussion

Syntheses: Initially we investigated the three different routes (1)–(3) as described in Scheme 1 to obtain access to a simple salt of $M^+[(RO)_3Al\text{-}F\text{-}Al(OR)_3]^-$ that may be used for metathesis reactions (M^+ = Cs^+, Tl^+ or Ag^+).

None of the routes shown in Scheme 1 led to success. In the course of reaction (1), which was performed in THF, we isolated the Lewis acid base adduct $Al(OR)_3\cdot(THF)$, **1**. The coordinative Al–O bond in **1** is so strong that the THF molecule is not even released in the vacuum of a diffusion pump (10^{-5} mbar). The dative Al–O bond in **1** (1.824(2) Å) is shorter than all other dative Al–O bonds from THF molecules (CSD search) and approaches distances usually found for covalent Al–O bonds. In agreement with this strong interaction we found that the THF molecule of **1** dissolved in CD_2Cl_2 is cleaved to the butoxide within 12 h (NMR). Reaction (2) performed in toluene or hexane at ambient temperatures led to decomposition of the donor free $Al(OR)_3$ intermediate, C–F bond activation, ionization and formation of salts that include Al-F-Al fluoride bridges prior to MF addition.[30] Reactions according to Equation (3) could not prevent C–F activation and led to decomposition with M = Ag^+.[31] In one reaction with CsF the alcohol R–OH was added to $AlMe_3$ at −78 °C and after addition of CsF the product of an incomplete substitution of Me for OR was obtained: $Cs^+[(RO)_2(Me)Al\text{-}F\text{-}Al(Me)(OR)_2]^-$ (X-ray, IR, NMR).

Reactions according to Equations (1)–(3) in Scheme 1 clearly demonstrate that the $Al(OR)_3$ intermediate is not simple to obtain. If kept at low temperatures the substitution reaction is not complete and if done at RT the obtained $Al(OR)_3$ Lewis acid is very strong and decomposes with fluoride ion abstraction. Thus it is not straight forward to employ $Al(OR)_3$ for further syntheses such as the preparation of the fluoride bridged $[(RO)_3Al\text{-}F\text{-}Al(OR)_3]^-$ anion.

Surprisingly we found a suitable and simple access to $Ag^+[(RO)_3Al\text{-}F\text{-}Al(OR)_3]^-$ during our continuing efforts to prepare novel binary P–X cations (X = halogen) [Eqs. (4) and (5)].

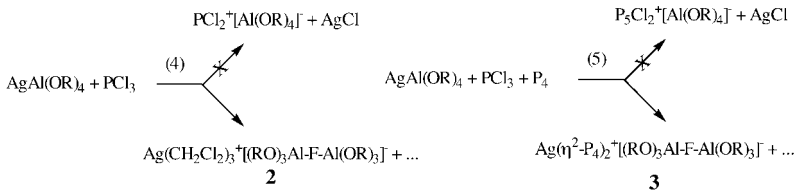

When trying to prepare PCl_2^+ and $P_5Cl_2^+$ cations similarly to our published procedure for $P_2X_5^+$ and $P_5X_2^+$ (X = Br, I)[29] from $Ag[Al(OR)_4]$, PCl_3 and P_4 according to Equations (4) and (5) at low temperatures (−78 to −30 °C) no or only very little AgCl precipitation was observed. Therefore we allowed the mixtures to warm to ambient temperature. After minutes the characteristic AgCl precipitate formed and was complete after stirring at RT for 4 to 5 d. To our surprise the filtrate of both suspensions contained exclusively the $Ag(CH_2Cl_2)_3^+[(RO)_3Al\text{-}F\text{-}Al(OR)_3]^-$ **2** and $Ag(\eta^2\text{-}P_4)_2^+[(RO)_3Al\text{-}F\text{-}Al(OR)_3]^-$ **3** salts (NMR) which were isolated in 84 and 86 % yield (based on Al) and fully characterized (see below). At 10^{-3} mbar one may remove all three coordinated CH_2Cl_2 molecules of 7 g of **2** within 48 h (NMR in $CDCl_3$).

Only once we found direct evidence for the intermediate formation of PCl_2^+ as shown in Equation (5): When the $PCl_3/Ag[Al(OR)_4]/P_4$ mixture was dissolved in CH_2Cl_2 and allowed to reach room temperature over night but subsequently stored at −28 °C, crystals of $Ag(P_4)_2^+[Al(OR)_4]^-$ and $Ag(P_4)_2^+[(RO)_3Al\text{-}F\text{-}Al(OR)_3]^-$ precipitated from the very concentrated solution (unit cell determinations). The remaining oil was analyzed by NMR and showed the singlet of PCl_3, that of coordinated P_4 at $\delta(^{31}P) = 492.9$ (approx. 90 % of the total signal intensity) but also three multiplets

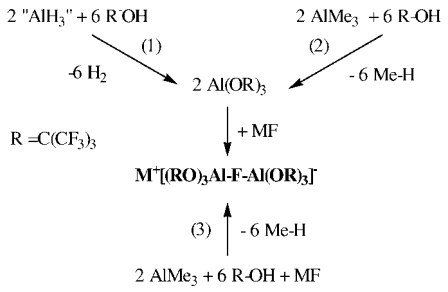

Scheme 1. Unsuccessful attempts to prepare $M^+[(RO)_3Al\text{-}F\text{-}Al(OR)_3]^-$ salts (M = Cs, Tl, Ag).

at $\delta^{31}P = 142.7$ (dt), 57.8 (tt) and −270.5 (td) that clearly indicated the formation of $P_5Cl_2^+$ from a short lived PCl_2^+ cation and P_4 at intermediate temperatures.

^{31}P NMR Characterization of $P_5Cl_2^+$: The $P_5Cl_2^+$ cation is the third known member of the series of $P_5X_2^+$ cations after the initial observation of X = I[18a] and X = Br[18b,29] (Figure 1). However, despite repeated attempts, we never succeeded in obtaining a pure $P_5Cl_2^+$ salt and the only evidence for the latter cation is the informative NMR spectrum (Table 1, original spectrum deposited).

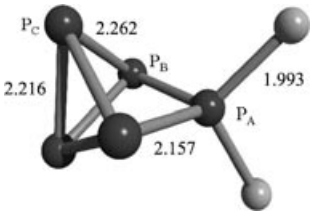

Figure 1. Structure and nomenclature of the P atoms of the C_{2v}-symmetric $P_5X_2^+$ cations (X = I, Br, Cl). Structural parameters of $P_5Cl_2^+$ optimized with MP2/TZVPP [Å].

Table 1. ^{31}P NMR shifts [ppm] and coupling constants [Hz] of all known $P_5X_2^+$ cations (X = I, Br, Cl); nomenclature of the P atoms as in Figure 1.

	$\delta^{31}P_A$	$\delta^{31}P_B$	$\delta^{31}P_C$	$^1J(P_{AB})$	$^1J(P_{BC})$
$P_5Cl_2^+$	57.8	142.7	−270.5	339.6	144.7
$P_5Br_2^+$	20.5	161.4	−235.9	320.4	149.1
$P_5I_2^+$	−89.0	168.2	−193.9	385.5	152.6

The trends of the chemical shifts when exchanging I for Br and Cl are very consistent throughout and lead to higher frequencies for the formal phosphonium center P_A but to lower frequencies for the remaining P_B and P_C atoms. The high frequency shift is influenced by less relativistic contribution[32] in going from I to Br and Cl just as the chemical shift of PX_4^+ decreases from −475 (I) to −80 (Br) and +83 ppm (Cl).[29,33]

Crystal structures: Details of the data collections and the crystal structure refinements are collected in Table 9 at the end of this article.

Al(OR)$_3$·(THF) (1): The core of this molecule consists of a distorted AlO_4 tetrahedron with three Al−O single bonds at about 1.71 Å and a dative Al−O bond to the THF-molecule at 1.824(2) Å (Figure 2). Compared to the homoleptic $[Al(OR)_4]^-$ anion,[20] the Al−OR bonds are shortened by about 0.015 Å and the average Al-O-C bond angle of 150.7° is slightly widened (by 1°). The dative Al−O bond in **1** is very short and according to a search of the CSD it comprises the shortest dative Al−O bond involving a THF molecule currently known. Thus, although the $C(CF_3)_3$ ligand is rather bulky and the sum of the RO−Al−OR bond angles is 343.1° (ideal tetrahedron: 328.5°), all Al−O distances are very short, indicating an electron deficient and highly Lewis acidic aluminum center in **1**.

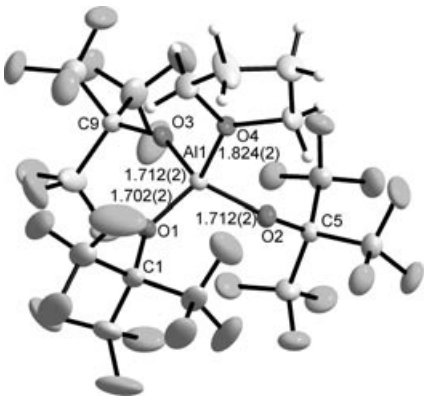

Figure 2. Section of the crystal structure of Al(OR)$_3$·(THF) **1** (R = C(CF$_3$)$_3$) at 150 K with thermal displacement ellipsoids showing 25% probability. The Al−O distances [Å] are given in the figure, other selected bond lengths [Å] and bond angles [°]: C1−O1 1.369(3), C5−O2 1.356(3), C9−O3 1.348(3), Al1-O1-C1 150.1(2), Al1-O2-C5 151.9(2), Al1-O3-C9 150.0(2), O1-Al1-O2 115.9(1), O1-Al1-O3 111.1(1), O2-Al1-O3 116.1(1).

Cs$^+$[(RO)$_2$(Me)Al-F-Al(Me)(OR)$_2$]$^-$: The asymmetric unit of the crystal structure of the fluoride bridged cesium aluminate is shown in Figure 3. Two formally neutral $(RO)_2AlMe$ moieties coordinate to a fluoride ion and are connected via a symmetric slightly bent Al-F-Al fluoride bridge (152.3°) with Al−F distances of about 1.80 Å. Each Al atom bears one methyl group at d(Al−C) ≈ 1.92 Å and two OR groups with Al−O separations of 1.73 to 1.75 Å. The negative charge of the aluminate is compensated by a twelve-fold weakly coordinated Cs^+ cation (9 Cs−F contacts, 3.361 Å on average, and 3 Cs−O contacts, 3.420 Å, on average).

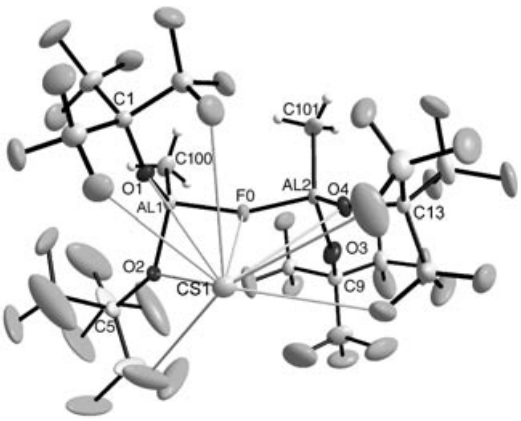

Figure 3. Section of the crystal structure of $Cs^+[(RO)_2(Me)Al\text{-}F\text{-}Al(Me)(OR)_2]^-$ (R = C(CF$_3$)$_3$) at 150 K with thermal displacement ellipsoids showing 25% probability. Selected bond lengths [Å] and bond angles [°]: Al1−F0 1.811(3), Al2−F0 1.791(3), Al1−C100 1.927(7), Al2−C101 1.917(6), Al1−O1 1.744(4), Al1−O2 1.743(4), Al2−O3 1.725(4), Al2−O4 1.745(4); Cs1−F0 3.241(3); Al1-F0-Al2 152.3(2), Al1-O1-C1 144.8(4), Al1-O2-C5 141.4(4), Al2-O3-C9 153.5(5), Al2-O4-C13 138.3(3); CN(Cs1) = 12, $d(Cs\text{-}F)_{range}$ = 3.224(6) to 3.568(5), average of the 9 Cs−F contacts: 3.361 Å, $d(Cs\text{–}O)_{range}$ = 3.352(4) to 3.458(4), average of the 3 Cs−F contacts: 3.420 Å. For clarity, 3 Cs−F contacts to other $[(RO)_2(Me)Al\text{-}F\text{-}Al(Me)(OR)_2]^-$ anions in the crystal lattice are not shown.

Compared with the fluoride bridged $[(RO)_3Al\text{-}F\text{-}Al(OR)_3]^-$ anion below, the Al–F bridging distances and the terminal Al–O distances are elongated in the cesium aluminate by about 0.03 to 0.05 Å. Although the $[(RO)_3Al\text{-}F\text{-}Al(OR)_3]^-$ anion is more crowded than the cesium aluminate (6 vs. 4 RO ligands), its Al–O and Al–F distances are substantially shorter. This is attributed to the substitution of two very electronegative OR ligands for the less electronegative Me-groups and indicates less electrophilic aluminum centers in the sterically less congested cesium aluminate structure that lead to longer and less polar bonds.

$Ag(CH_2Cl_2)_3^+[(RO)_3Al\text{-}F\text{-}Al(OR)_3]^-$ (2) and $Ag(\eta^2\text{-}P_4)_2^+[(RO)_3Al\text{-}F\text{-}Al(OR)_3]^-$ (3): In the solid state **2** and **3** form ionic lattices with well separated cations and anions. The Ag atoms in the cations show interactions to the ligands CH_2Cl_2 and P_4, but not to the anions. All Ag–F distances are longer than 3.40 Å. Drawings of **2** and **3** are shown in Figures 4 and 5.

The silver atom in **2** is coordinated by six Cl atoms of the CH_2Cl_2 molecules at 2.661(2) to 2.836(2) Å (average: 2.752 Å; Figure 4b). The Ag–Cl distances in **2** are similar to those found earlier for $(H_2CCl_2)AgAl(OC(Me)(CF_3)_2)_4$ (2.613(2) to 2.874(2) Å) or $Ag(1,2\text{-}Cl_2C_2H_4)_3^+[Al(OR)_4]^-$ (2.694(2) to 2.788(2) Å; average: 2.742 Å).[20] In contrast to the structure[34] of $(Ag(CH_2Cl_2)_3^+)_2[Ti(OTeF_5)_6]^{2-}$ with a clearly eight-fold coordination of the silver atom by six chlorine atoms at 2.66 to 3.04 Å (average: 2.84 Å) and two fluorine atoms from the anion at 3.03 Å (Figure 4c), the silver atom in **2** exhibits no extra contacts to the anion (Figure 4b). This shows that the $[(RO)_3Al\text{-}F\text{-}Al(OR)_3]^-$ anion is less coordinating than the $[Ti(OTeF_5)_6]^{2-}$ anion. Therefore, $Ag(CH_2Cl_2)_3^+$ is the first true homoleptic metal-CH_2Cl_2 cation without extra cation–anion contacts.

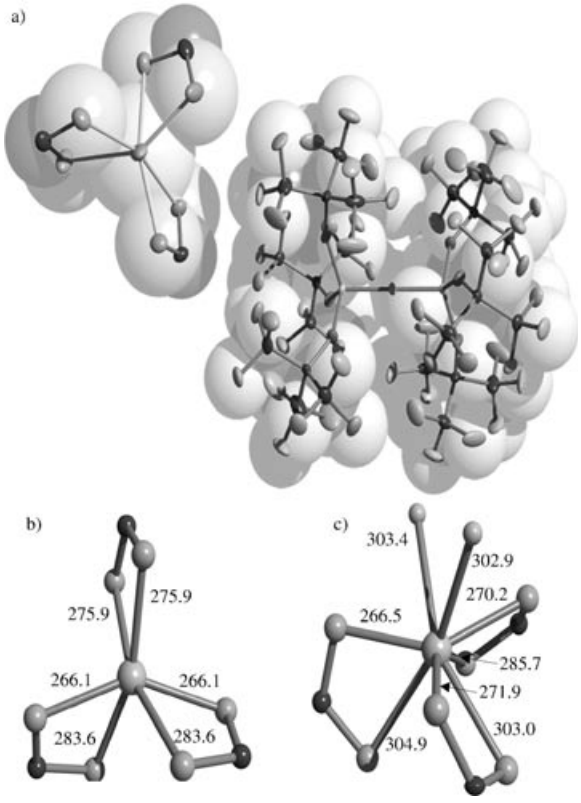

Figure 4. a) Section of the crystal structure of $Ag(CH_2Cl_2)_3^+[(RO)_3Al\text{-}F\text{-}Al(OR)_3]^-$ **2** (R = $C(CF_3)_3$) at 150 K with thermal displacement ellipsoids showing 25% probability. Hydrogen atoms were omitted. Superposition with a space filling model. b) $AgCl_6$ coordination in **2**. c) $AgCl_6F_2$ coordination in $(Ag(CH_2Cl_2)_3^+)_2[Ti(OTeF_5)_6]^{2-}$.[34]

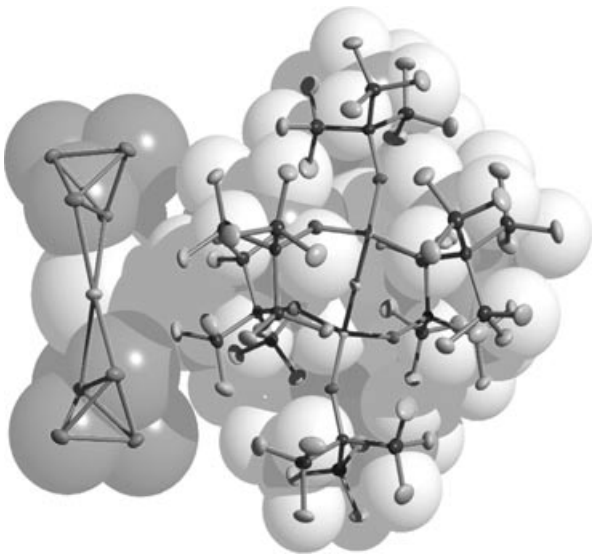

Figure 5. Section of the crystal structure of $Ag(\eta^2\text{-}P_4)_2^+[(RO)_3Al\text{-}F\text{-}Al(OR)_3]^-$ (R = $C(CF_3)_3$) at 150 K with thermal displacement ellipsoids showing 25% probability. Superposition with a space filling model.

The structural parameters of the centrosymmetric $Ag(\eta^2\text{-}P_4)_2^+$ cation in **3** resemble those observed in the $[Al(OR)_4]^-$ salt[14] within 0.002 Å (Table 2). However, in the almost D_2-symmetric $Ag(\eta^2\text{-}P_4)_2^+$ cation in **3** the two AgP_2 planes include an angle of 44.2°, while this interplanar angle in $Ag(\eta^2\text{-}P_4)_2^+[Al(OR)_4]^-$ amounts to 10.6 (at 150 K) and 0° (at 200 K). Thus the latter $Ag(\eta^2\text{-}P_4)_2^+$ cation is best described as being almost D_{2h}-symmetric.[14] The $Ag(\eta^2\text{-}P_4)_2^+$ cations in both salts are compared in Table 2.

Since the structure of $Ag(\eta^2\text{-}P_4)_2^+[Al(OR)_4]^-$ showed a considerable temperature dependence of the interplanar angle of the two AgP_2 planes, we also recorded a data set for **3** at 200 K. However, the structure remained identical within the error limits. A drawing of the 12 weak P–F cation–anion contacts between 3.248 and 3.393 Å (av.

Table 2. Comparison of the structural parameters of the $Ag(\eta^2\text{-}P_4)_2^+$ cation as $[Al(OR)_4]^-$ and $[(RO)_3Al\text{-}F\text{-}Al(OR)_3]^-$ salts at 150 K (R = $C(CF_3)_3$).

Parameter	$[Al(OR)_4]^-$	$[(RO)_3Al\text{-}F\text{-}Al(OR)_3]^-$
d(Ag–P_{Ag}) [Å]	2.536(1)–2.548(1) av. 2.541	2.538(1)–2.540(1) av. 2.539
d(P_{Ag}–P_{Ag}) [Å]	2.328(2)–2.330(2) av. 2.329	2.330(1)
d(P_{Ag}–P) [Å]	2.145(2)–2.163(2) av. 2.154	2.156(1)–2.161(1) av.: 2.159
d(P–P) [Å]	2.172(2)–2.174(2) 2.173	2.195(1)
$\sphericalangle$(P-P-P)$_{range}$ [°]	56.89(7)–65.53(7)	57.30(4)–65.35(4)
$\sphericalangle$(AgP_2)[a] [°]	10.6	44.2

[a] Interplanar angle between the two AgP_2 planes.

3.331 Å) is deposited. The structures of the $[(RO)_3Al\text{-}F\text{-}Al(OR)_3]^-$ anions in **2** and **3** are discussed below.

Quantum chemical calculations: To assign the vibrational frequencies and the NMR shifts of the $[(RO)_3Al\text{-}F\text{-}Al(OR)_3]^-$ anion with confidence and to understand the mechanism of the formation of **2** and **3** all possibly important species were calculated at the BP86/SV(P) (DFT) and partially also at the MP2/TZVPP ab initio level. The total energies, zero point energies (ZPE), COSMO solvation enthalpies as well as thermal and entropic contributions to the Gibbs free energy are collected in Table 3. The DFT-optimized structures of $Al(OR)_3$, $[F\text{-}Al(OR)_3]^-$, $[Al(OR)_4]^-$ and $[(RO)_3Al\text{-}F\text{-}Al(OR)_3]^-$ were taken from earlier work and are fully described elsewhere,[35] however, the vibrational frequencies and NMR shifts are reported for the first time herein.

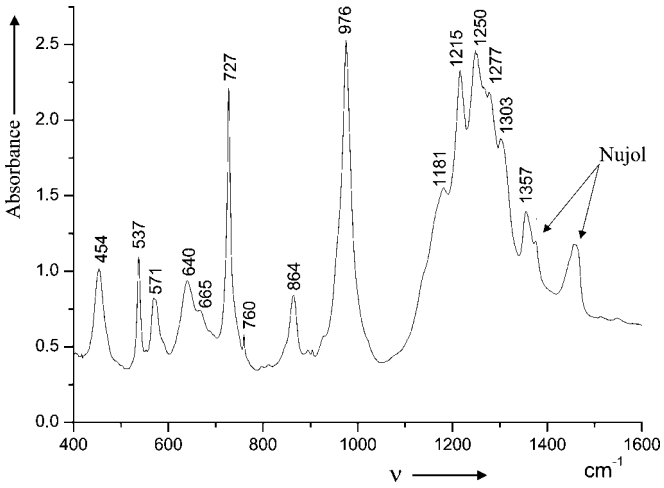

Figure 6. IR Spectrum of a nujol mull of **2** between CsI plates in the range of 400 to 1600 cm^{-1}.

Table 3. The total energies at the BP86/SV(P) and partially also MP2/TZVPP levels, zero point energies (ZPE, BP86/SV(P) quality), COSMO solvation enthalpies ($\varepsilon_{rel}=8.93$) as well as thermal and entropic contributions G(298 K) to the Gibbs free energy of all compounds used to establish the mechanism of the formation of **2** and **3** in Scheme 2. All values are given in Hartree.

R = $C(CF_3)_3$	BP86/SV(P) (U(0 K))	ZPE	COSMO	G(298 K)	MP2/TZVPP
$Al(OR)_3$	−3618.91753	0.18692	−0.00272	0.11504	–
$Al(OR)_4^-$	−4744.54880	0.24459	−0.04035	0.15665	–
$RO_3Al\text{-}F\text{-}AlOR_3^-$	−7337.85243	0.37050	−0.03516	0.25959	–
$FAl(OR)_3^-$	−3718.87659	0.18745	−0.04680	0.11587	–
C_4F_8	−950.47604	0.04615	−0.00299	0.01797	−949.95719
OC_4F_8	−1025.63918	0.05012	−0.00178	0.01894	−1025.07370
PCl_3	−1721.67144	0.00453	−0.00215	−0.02497	−1720.05658
PCl_2^+	−1261.19840	0.00314	−0.08766	−0.02427	−1259.98572
$ROPCl_2$	−2387.00015	0.05789	−0.00217	0.01853	−2385.20193
Ag^+	−146.75968	0	−0.09779	−0.01661	−146.21682
AgCl	−607.21036	0.00077	−0.01530	−0.02378	−606.23344

To account for the formation of solid AgCl the enthalpy of sublimation of $AgCl_{(s)}$ of 231 kJ mol^{-1} was included in the calculations.[36]

Infrared spectrum of 2: A representative IR spectrum of **2** is shown in Figure 6. The anion bands are collected in Table 4 and compared with the BP86/SV(P) calculated frequencies of the $[(RO)_3Al\text{-}F\text{-}Al(OR)_3]^-$ anion as well as with the experimental $[Al(OR)_4]^-$ anion bands of the $NEt_4^+[Al(OR)_4]^-$ salt.

Infrared spectra of several batches of **2** were recorded. However, no evidence for bands that may be assigned to the $Ag(CH_2Cl_2)_3^+$ cation were observed, possibly due to their weak (BP86/SV(P) calculated) IR intensities of only 0 to 25 km mol^{-1} (Table deposited). The only exception from this notion refers to two bands calculated to occur at 677 and 688 cm^{-1}. However, this is an area of intense absorptions of the anion and the only experimental band that may be attributed to one of these calculated frequencies is a shoulder at 665 cm^{-1}. All other cation bands are either too weak or obscured by the anion. Therefore the spectrum in Figure 6 represents almost exclusively anion bands (see Table 4).

The agreement between calculated and experimental anion bands is very good and the comparison to the homoleptic $NEt_4^+[Al(OR)_4]^-$ salt shows only two differences that can be used to differentiate between samples or mixtures of the two anions: the bands at 640 and 864 cm^{-1}. The first can be assigned to the Al–F stretching vibration of the Al-F-Al moiety in **2** and is, therefore, absent in $[Al(OR)_4]^-$ salts. Its position may be compared with the Al-F-Al stretches in $(Me_2AlF)_4$ at 638 and 614 cm^{-1}.[37] For the band at 864 cm^{-1} the respective mode in the $[Al(OR)_4]^-$ salts is always found around 832 ±

Table 4. Experimental bands of **2** and calculated frequencies of the $[(RO)_3Al\text{-}F\text{-}Al(OR)_3]^-$ anion; comparison with the $[Al(OR)_4]^-$ anion bands of the $NEt_4^+[Al(OR)_4]^-$ salt [cm^{-1}].

$NEt_4^+[Al(OR)_4]^-$	**2**	calcd $[(RO)_3Al\text{-}F\text{-}Al(OR)_3]^-$
286 (mw)	295 (w)	280 (w) + 289 (w)
316 (m)	318 (w)	304 (w)
331 (w)	331 (vw)	319 (w)
367 (mw)	–	352 (w)
378 (mw)	374 (w)	367 (m) + 385 (w)
447 (ms)	454 (m)	445 (m)
537 (m)	537 (m)	520 (m)
562 (m)	–	–
571 (m)	571 (m)	559 (m)
–	640 (m)	637 (m)
–	665 (sh, ?[a])	–
727 (s)	727 (s)	709 (s)
756 (mw)	760 (mw)	–
833 (m)	–	–
–	862 (ms)	847 + 856 (m)
973 (s)	975 (s)	964 (s)
–	1150 (sh, ?)	1144 (mw)
1217 (vs)	1181 (sh)	1192 (mw)
1240 (s)	1215 (s)	1210 (s)
1254 (s)	1250 (vs)	1237 (vs)
1277 (vs)	1277 (vs)	1261 (s)
1299 (s)	1303 (s)	1333 (s)
1353 (ms)	1357 (s)	1345 (m)

[a] $Ag(CH_2Cl_2)_3^+$?

4 cm^{-1} and this difference of about 30 cm^{-1} also allows to distinguish between $[Al(OR)_4]^-$ and $[(RO)_3Al\text{-}F\text{-}Al(OR)_3]^-$ salts.

NMR Spectra of the $[(RO)_3Al\text{-}F\text{-}Al(OR)_3]^-$ anion: The most drastic change of the NMR spectra of the $[(RO)_3Al\text{-}F\text{-}Al(OR)_3]^-$ anion in comparison with those of $[Al(OR)_4]^-$ occurs in the ^{27}Al NMR: the homoleptic anion always shows very sharp resonances at $\delta^{27}Al = 34$ to 39 ppm with half widths of 6 to 130 Hz. The position of the ^{27}Al NMR shift of the fluoride bridged anion is similar (34 ppm). However, the half width increases by a factor of at least 17 to about 2200 Hz (Figure 7).

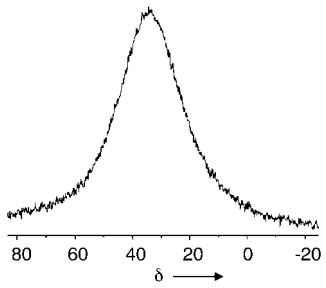

Figure 7. ^{27}Al NMR spectrum of the $[(RO)_3Al\text{-}F\text{-}Al(OR)_3]^-$ anion.

Small impurities of the homoleptic $[Al(OR)_4]^-$ anion in the sample always lead to broad signals which bear a small sharp signal due to $[Al(OR)_4]^-$ on top of it. Therefore the broad signal of $[(RO)_3Al\text{-}F\text{-}Al(OR)_3]^-$ provides clear evidence for a clean starting material. We also observed the bridging fluoride in the $[(RO)_3Al\text{-}F\text{-}Al(OR)_3]^-$ anion in **2** at $\delta^{19}F = -185$ (calcd -194). This value is close to those observed for other organometallic tetracoordinate Al-F-Al bridged compounds, that is, $\delta(^{19}F) = -159$ for the bridging F in $(RAl(F)(\mu\text{-}F))_2$ ($R = [(Me_3Si)N\text{-}C(Ph)(C(SiMe_3)_2]^-$).[38] All NMR data are collected in Table 5 and compared to the DFT calculated NMR shifts as well as the respective shifts in the homoleptic $[Al(OR)_4]^-$ anion.

Table 5. Typical NMR data of the $[(RO)_3Al\text{-}F\text{-}Al(OR)_3]^-$ anion compared to the DFT calculated NMR shifts as well as the respective shifts in the homoleptic $[Al(OR)_4]^-$ anion [experimental shifts in CD_2Cl_2 solution in ppm].

Moiety	$[(RO)_3Al\text{-}F\text{-}Al(OR)_3]$ (exptl	$[(RO)_3Al\text{-}F\text{-}Al(OR)_3]$ (calcd)	$[Al(OR)_4]^-$ (exptl)
Al	34 ($\Delta_{1/2}$ = 2200 Hz)	–	34–39 ($\Delta_{1/2}$ = 6–130 Hz)
$OC(CF_3)_3$	79 (broad)	85	80 (broad)
$OC(\boldsymbol{C}F_3)_3$	121.0 ($^1J_{CF}$ = 291 Hz)	131	121.5 ($^1J_{CF}$ = 293 Hz)
$OC(C\boldsymbol{F}_3)_3$	−75.3	−88 to −91	−76.0
Al-***F***-Al	−184.6	−194	–

Also the small but always reproducible difference between the ^{13}C NMR shifts of the CF_3 groups in both anions of $\Delta(\delta^{13}C) = 0.5$ can be used as a diagnostic for the elucidation whether the bridged or the homoleptic anion is present in the sample.

A possible mechanism for the formation of the fluoride bridged anion: As seen above from the formation of the $P_5Cl_2^+$ cation in the course of the preparation of **3**, one may assume that initially a PCl_2^+ cation formed by reaction of Ag^+ with PCl_3. To understand the mechanism of the formation of **2** and **3** we will therefore start to summarize the properties of this very reactive player before suggesting a likely mechanism.

The PCl_2^+ cation: This species is well known in the gas phase, but no reports on the presence of isolated PCl_2^+ in condensed phases exist. In the gas phase it was shown that PCl_2^+ abstracts fluoride from perfluorocyclohexane[39] and cleaves cyclic ethers. The first step of this cleavage was shown to be the addition of the phosphenium ion to the oxygen atom of the ether giving $Cl_2P\text{-}OR_2^+$.[40] Thus PCl_2^+ is very reactive and cleaves even the very stable C–F bonds in perfluorocyclohexane, but still may act as a Lewis acid and coordinates oxygen-donors. Computational work by Gudat[41] showed that the PCl_2^+ cation is a true electrophilic carbene analogue in which the largest lobe of the HOMO is centered on the P atom (and not on the heteroatoms such as in $P(NH_2)_2^+$). Formally the PX_2^+ cations may be viewed as being π-bonded with the MOs shown in Figure 8. The better the backbonding from the halogen or other heteroatoms X in PX_2^+, the more stable is PX_2^+. Consequently many heteroatoms stabilized PX_2^+ cations with $X = NR_2$ or SR are known,[42] but reports on phosphenium ions with X = F, Cl are restricted to the gas phase, while we presented reasonable evidence to assume the formation of long lived PBr_2^+ and PI_2^+ intermediates in CH_2Cl_2 solution at low temperatures.[18b,29] This is in line with the fluoride ion affinity (FIA)[43] of the gaseous PX_2^+ cation, the partial charges that reside on the P atom as well as the shared electron numbers of the P–X bonds with X = F–I collected in Table 6. For comparison the FIA values of CX_3^+ (X = F–I)[19] are also included.

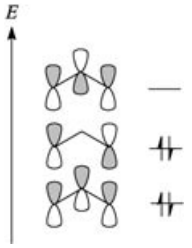

Figure 8. π-MOs of PX_2^+.

From the FIA values in Table 6 one notes that the heavier PX_2^+ cations (X = Cl–I) are considerably more reactive than the heavier CX_3^+ carbenium ions of which the CI_3^+ $[Al(OR)_4]^-$ salt dissolved in CH_2Cl_2 is stable at room temperature for days.[19] In PF_2^+

Table 6. FIA of PX_2^+ and CX_3^+ [kJ mol^{-1}], partial charges residing on the P atom in PX_2^+ $q(P)$ and shared electron numbers (SEN) of the P–X bond obtained by MP2/TZVPP. The FIA values in parenthesis include the solvation enthalpies as calculated by COSMO for CH_2Cl_2 as a solvent.

X	FIA(PX_2^+)	FIA(CX_3^+)[19]	$q(P)$	SEN P–X
F	1087 (480)	1099 (497)	1.18	1.27
Cl	1003 (445)	904 (359)	0.82	1.38
Br	973 (431)	871 (343)	0.73	1.35
I	920 (395)	813 (302)	0.39	1.38

and PCl_2^+ approximately a +1 charge resides on the P atom.

From the preceding follows: PF_2^+ is the most reactive PX_2^+ cation, but still PCl_2^+ is substantially more reactive than PBr_2^+, PI_2^+, CCl_3^+, CBr_3^+ and CI_3^+, all of which could be handled[19,29,44] under conditions where the PCl_2^+ intermediate immediately reacted with the counterion.

Formation of $[(RO)_3Al\text{-}F\text{-}Al(OR)_3]^-$: Our suggestion for anion decomposition and formation of the fluoride bridged anion is presented in Scheme 2. The mechanism is hypothetical; however, it agrees with all experimentally available results as well as quantum chemical calculations including solvation and entropy effects.

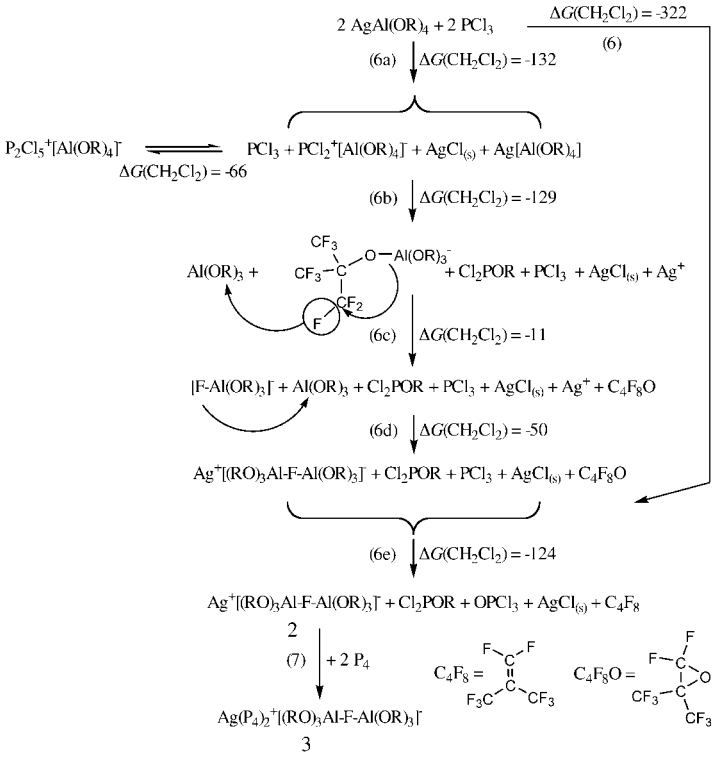

Scheme 2. Hypothetical mechanism for the formation of **2** and **3**. The calculated Gibbs energies ΔG in CH_2Cl_2 solution are given at 298 K in kJ mol^{-1}.

The initially formed PCl_2^+ cation presumably reacts with excess PCl_3 and is in equilibrium with $P_2Cl_5^+$. We already showed for the analogous $P_2Br_5^+$ cation[29] that the latter is an effective PBr_2^+ donor in solution. Therefore, the PCl_2^+ present in the equilibrium will react with the $[Al(OR)_4]^-$ anion with abstraction of OR^- and formation of Cl_2POR (see reaction with ether[40] above). The $Al(OR)_3$ Lewis acid thus formed then activates one of the 36 equivalent C–F bonds of another $[Al(OR)_4]^-$ anion and forms $[F\text{-}Al(OR)_3]^-$ and the epoxide C_4F_8O (as also seen in the reaction of $AlMe_3$ with 3 ROH above). This reaction is supported by the formation of a new C–O bond in C_4F_8O. After dissociation of the initially coordinated weak base C_4F_8O, the $[(RO)_3Al\text{-}F\text{-}Al(OR)_3]^-$ anion formed by combination of $[F\text{-}Al(OR)_3]^-$ with $Al(OR)_3$. In the final step C_4F_8O acts as an oxygen donor that oxidizes the excess PCl_3 to $OPCl_3$ which is stable against Cl^- abstraction and precipitation of AgCl.[45] Also, $ROPCl_2$ is (kinetically?) stable against Cl^- abstraction. If, as in reaction (5), P_4 is present in the solution, this reagent, now available in the right stoichiometric amount, coordinates to Ag^+ and forms **3** (Eq. (7) in Scheme 2). After filtration from the insoluble AgCl and removal of all volatiles in vacuo (CH_2Cl_2, C_4F_8 und $OPCl_3$) **2** and **3** are obtained in good yield. This postulated mechanism is in agreement with the formation of **2** and **3**, the mass balance of the reaction leading to **2**, the elemental analysis of **2**, as well as the by-products Cl_2POR [decet at $\delta^{31}P(-80\,°C) = -214.6$ ($^3J_{PF} = 28.5$ Hz] and C_4F_8O [$\delta^{19}F(-80\,°C) = -69.2$ (s, CF_3), -108.3 (s, CF_2)] observed in in situ NMR experiments of reaction (4) in CD_2Cl_2 solution.

Investigation of the stability of the $[(RO)_3Al\text{-}F\text{-}Al(OR)_3]^-$ anion: An analysis of the structural parameters of the $[(RO)_3Al\text{-}F\text{-}Al(OR)_3]^-$ anion clearly shows that it is more stable against ligand abstraction than the homoleptic $[Al(OR)_4]^-$ anion. Thus the average Al–O distance in $[Al(OR)_4]^-$ is 1.725 Å, while it shrunk in $[(RO)_3Al\text{-}F\text{-}Al(OR)_3]^-$ by 0.027 to 0.036 Å to about 1.695 Å (Table 7).

Comparison to the closely related and sterically less crowded anion in $Cs^+[(RO)_2(Me)Al\text{-}F\text{-}Al(Me)(OR)_2]^-$ (CsX) with 0.03 to 0.04 Å longer Al–O and Al–F bonds shows that the very short Al–O and Al–F distances in the $[(RO)_3Al\text{-}F\text{-}Al(OR)_3]^-$ anion are due to the very electrophilic and highly Lewis acidic Al centers which stabilize the anion against ligand abstraction. In agreement with this we recently prepared PI_4^+, CI_3^+ and other reactive cation salts starting from **2**.[31,44] From the space filling models of $[Al(OR)_4]^-$ and $[(RO)_3Al\text{-}F\text{-}Al(OR)_3]^-$ shown in Figure 9 one notes that the oxygen atoms in the fluoride bridged anion are less accessible. Therefore, they are not available for coordination as the starting point for anion decomposition as those of $[Al(OR)_4]^-$ in Scheme 2.

In contrast to the less crowded $[(RO)_2(Me)Al\text{-}F\text{-}Al(Me)(OR)_2]^-$ anion also the bridging fluoride is complete-

Table 7. Comparison of the structural parameters of the $[(RO)_3Al\text{-}F\text{-}Al(OR)_3]^-$ anions in **2** and **3** with those of $P_2I_5^+[(RO)_3Al\text{-}F\text{-}Al(OR)_3]^-$,[29] $Cs^+[(RO)_2(Me)Al\text{-}F\text{-}Al(Me)(OR)_2]^-$ (CsX) and $[Al(OR)_4]^-$ as $Ag(Cl_2C_2H_4)_3^+$ salt.[20]

Parameter	$P_2I_5^+$[a]	**2**	**3**	CsX[b]	$Al(OR)_4^-$
d(Al–O)$_{range}$ [Å]	1.681(6)–1.694(5)	1.691(3)–1.701(3)	1.696(2)–1.699(2)	1.725(4)–1.745(4)	1.714(3)–1.736(3)
d(Al-O)$_{av.}$ [Å]	1.689	1.697	1.698	1.739	1.725
∢(Al-O-C)$_{av.}$ [°]	153.1	150.5	151.1	144.5	149.5
d(Al–F)$_{range}$ [Å]	1.764(2)–1.775(2)	1.769(1)	1.7654(7)	1.791(3)–1.811(3)	–
d(Al–F)$_{av.}$ [Å]	1.770	–	–	1.801	–
∢(Al-F-Al) [°]	180	180	180	152.3	–

[a] In $P_2I_5^+[(RO)_3Al\text{-}F\text{-}Al(OR)_3]^-$.[29] [b] CsX = $Cs^+[(RO)_2(Me)Al\text{-}F\text{-}Al(Me)(OR)_2]^-$.

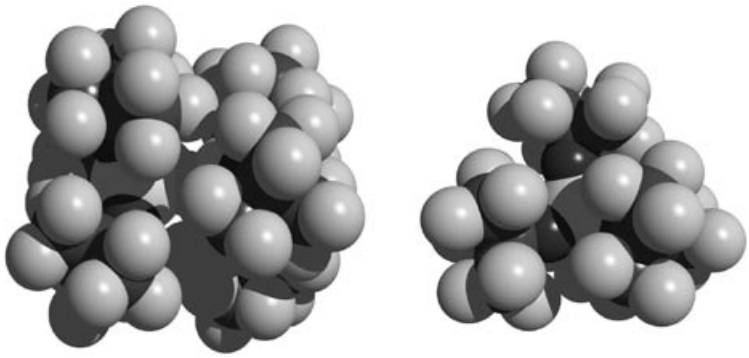

Figure 9. Comparison of the space filling models of $[Al(OR)_4]^-$ and $[(RO)_3Al\text{-}F\text{-}Al(OR)_3]^-$ ($R = C(CF_3)_3$). One should note the better steric shielding of the most basic oxygen atoms in the fluoride bridged anion.

ly covered by CF_3 groups and not available for coordination and/or decomposition. This notion is in agreement with the known strengths of the Al–F bond as well as the fluoride ion affinity (FIA)[43] of two molecules of $Al(OR)_3$ (685 kJ mol^{-1}).[35,43,46] This value was calculated in analogy to the FIA[47] value of gaseous SbF_5 of 503 kJ mol^{-1}. The calculated FIA value of $2\,Al(OR)_3$ represents the highest known FIA. It is even higher than the FIA of monomeric AuF_5, recently calculated by Seppelt et al. as 590 kJ mol^{-1}.[48] In analogy to $[Sb_2F_{11}]^-$, which is considerably more stable towards fluoride abstraction than $[SbF_6]^-$, the $[(RO)_3Al\text{-}F\text{-}Al(OR)_3]^-$ anion is also more stable towards electrophiles than the $[Al(OR)_4]^-$ anion. The fact that $2\,Al(OR)_3$ is a stronger Lewis acid than $2\,SbF_5$ may also be shown in the following isodesmic reaction (8) calculated by BP86/SV(P):

$$2\,Al(OR)_3 + Sb_2F_{11}^- \xrightarrow{\Delta_r H = -40\ kJ\ mol^{-1}} (RO)_3Al\text{-}F\text{-}Al(OR)_3^- + 2\,SbF_5 \quad (8)$$

Equation (8) shows that the F^- affinity of the Lewis acid $2\,Al(OR)_3$ is by 40 kJ mol^{-1} higher than that of $2\,SbF_5$. This very high FIA of $2\,Al(OR)_3$ is the reason for the instability and high reactivity nature of the $Al(OR)_3$ Lewis acid that was generated in situ from $AlMe_3$ and 3 ROH.[30,31] Further DFT calculations showed[35] the stability of the $[(RO)_3Al\text{-}F\text{-}Al(OR)_3]^-$ anion as evidenced by the FIA, the ligand affinity LA,[49a] the anion decomposition in the presence of a hard (H^+, PD)[49b] or soft (Cu^+, CuD)[49b] electrophile, the HOMO level,[49c] the HOMO–LUMO gap[49d] and the partial charges of most negatively charged atoms[49e] taken from refs. [1d, 35] and collected in Table 8 in comparison to other WCAs.

According to each entry in Table 8 the fluoride bridged $[(RO)_3Al\text{-}F\text{-}Al(OR)_3]^-$ anion is among the very best WCAs.

On the ground state structure of the $Ag(\eta^2\text{-}P_4)_2^+$ cation: Figure 10 shows drawings of the structure of the $Ag(\eta^2\text{-}P_4)_2^+$ cation as $[Al(OR)_4]^-$ and $[(RO)_3Al\text{-}F\text{-}Al(OR)_3]^-$ salts. From this drawings we conclude that the symmetry of the ground state structure of the $Ag(\eta^2\text{-}P_4)_2^+$ cation (D_2, D_{2h} or D_{2d}) depends on temperature, weak P–F contacts and, most important, packing effects of the ions in the ionic lattice.

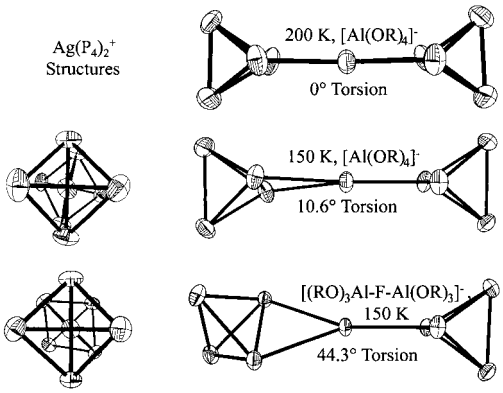

Figure 10. Temperature and anion dependence of the orientations of the $Ag(\eta^2\text{-}P_4)_2^+$ cations ($[Al(OR)_4]^-$ and $[(RO)_3Al\text{-}F\text{-}Al(OR)_3]^-$ salts).

This conclusion is in agreement with the calculated flat potential for a rotation of the P_4 tetrahedra around the Ag (P_2-centroid) vector.[14,50] Thus we could show for the first time on experimental grounds that several orientations of the $Ag(\eta^2\text{-}P_4)_2^+$ cation are very close in energy and that the finally realized geometry—D_2 or D_{2h}[14]—clearly depends on the solid state requirements of the packing of the ions. Also the related $[Au(P_3Mtppme)_2]^+PF_6^-$ (M = Co, Rh, Ir) contains a similar interplanar angle of 51° of the two η^2-P_3 cycles bonded to the Au atom.[51] This conclusion also shows

Table 8. Calculated properties of WCAs taken from refs. [1d, 35]. The FIA of the parent Lewis acid, the LA, PD and CuD of the WCA, the position of the HOMO of the WCA in eV, the HOMO–LUMO gap of the WCA in eV, the partial charge of the most negatively charged atom $q_{neg.}$, the partial charge of the most negatively charged surface atom $q_{surf.}$.

Anion	FIA [kJ mol^{-1}]	LA [kJ mol^{-1}]	PD [kJ mol^{-1}]	CuD [kJ mol^{-1}]	HOMO [eV]	Gap [eV]	$q_{neg.}$	$Atom_{neg.}$	$q_{surf.}$	$Atom_{surf.}$
$[Sb_4F_{21}]^-$ vs Sb_4F_{20}	584	[a]	−991	−301	−6.579	3.256	−0.39	F	−0.39	F
$[Sb(OTeF_5)_6]^-$	633	341	−973	−353	−6.610	2.326	−0.61	O	−0.39	F
$[Al(OR)_4]^-$ ($R = C(CF_3)_3$)	537	342	−1081	−395	−4.100	6.747	−0.24	O	−0.20	F
$[(RO)_3Al\text{-}F\text{-}Al(OR)_3]^-$ ($R = C(CF_3)_3$)[b]	685[b]	441	−983	−297	−4.987	6.500	−0.23	O	−0.20	F
$[B(C_6F_5)_4]^-$	444	296	−1256	−538	−3.130	4.196	−0.21	F	−0.21	F
$[B(CF_3)_4]^-$	552	490	−1136	−379	−3.530	9.158	−0.58	B	−0.21	F

[a] LA and FIA are identical. [b] FIA vs. 2 $Al(OR)_3$.

that back bonding from occupied $4d^{10}$ silver orbitals, as suggested by DFT calculations (40 to 60 kJ mol^{-1}),[14,50] is not structure determining, since in this case a clear structural preference for a 0 or 90° torsion angle would have been observed regardless which anion was used. This shows that the results of population analyses of quantum chemical DFT calculations for such weakly bound systems are at least debatable.

Conclusion and Outlook

In conclusion we note that the negative charge of the $[(RO)_3Al\text{-}F\text{-}Al(OR)_3]^-$ anion is dispersed over a "Teflon-surface" built from 54 peripheral C–F bonds. This anion contains 18 peripheral fluorine atoms more than all other currently known WCAs and, since the more basic oxygen atoms are no longer available for coordination due to steric reasons, it is the least coordinating anion currently known. Moreover, it is in almost every entry collected in Table 8 among the very best WCAs currently known. However, due to the methodology used, carborane based anions had to be excluded from Table 8. Of those anions only the $[CB_{11}(CF_3)_{12}]^-$ anion[25] is a close competitor of $[(RO)_3Al\text{-}F\text{-}Al(OR)_3]^-$ in terms of coordinating ability; in terms of stability towards reactive and simple cations the $[CB_{11}F_{12}]^-$ anion[24] or the $[CB_{11}Cl_6(R)_6]^-$ (R = H, CH_3) anions[23] are certainly superior. The presented simple preparation of the $Ag^+[(RO)_3Al\text{-}F\text{-}Al(OR)_3]^-$ **2** silver salt should lead to an application of this anion in all areas of chemistry where cation–anion interactions have to be rigorously minimized; that is below the coordination level provided by $[Al(OR)_4]^-$ or a related anion or when especially reactive cations not compatible with $[Al(OR)_4]^-$ or a related anion have to be stabilized.

Experimental Section

All manipulations were performed using standard grease free Schlenk or dry box techniques and a dinitrogen or argon atmosphere. Apparatus were closed by J. Young valves. CH_2Cl_2 was rigorously dried by five additions of 20 g portions of P_2O_5 over 4 d followed by distillation; it was degassed prior to use and stored under N_2. Yellow phosphorus was sublimed prior to use. The silver aluminate $Ag[Al(OR)_4]$ was prepared according to the literature.[20] FT-Raman spectra were obtained at r.t. from neat samples sealed under a dinitrogen atmosphere in dried melting point capillaries or 5 mm NMR tubes on a FT-IR spectrometer (Bruker IFS-66) equipped with a FT-Raman accessory (Bruker FRA-106) using a Nd-YAG laser (1064 nm irradiation, 4 cm^{-1} resolution). IR spectra were recorded on the same spectrometer in Nujol mull between CsI plates. NMR spectra of sealed samples were run on a Bruker AC250 spectrometer in CD_2Cl_2 and were referenced towards the solvent (^{1}H, ^{13}C) or external H_3PO_4 (^{31}P), $CFCl_3$ (^{19}F) and aqueous $AlCl_3$ (^{27}Al).

*THF·Al(OC(CF$_3$)$_3$)$_3$ **1**:* A 2.0 M solution of $Al(CH_3)_3$ in heptane (3.6 mL, 7.173 mmol) was added dropwise (2 h) to a cooled solution (0 °C) of $(CF_3)_3COH$ (3 mL, 21.519 mmol) in pentane (30 mL), while methane gas formed during the reaction. After addition of the $Al(CH_3)_3$, the solvent was evaporated leaving a yellow-brownish solid, insoluble in pentane as well as in CH_2Cl_2. Sublimation failed leaving a dark, nearly black solid. This residue was dissolved in THF and X-ray quality crystals were obtained from THF at −28 °C. Yield: 0.182 g (3.2 % with respect to nonafluorotertbutanol) as a crystalline compound. ^{1}H NMR (250 MHz, CD_2Cl_2, 25 °C): δ = 4.30 (m, 4H), 2.15 (m, 4H); ^{27}Al NMR (78 MHz, CD_2Cl_2, 25 °C): δ = 39.3 (s, $\tilde{\nu}_{1/2}$ = 624 Hz).

A more convenient route to **1** is the reaction of 3 equiv $LiAlH_4$ with $AlCl_3$ in THF at −78 °C ($\hat{=}$ 4 "AlH_3" + 3 LiCl) followed by quick addition of 12 equiv HO-C$(CF_3)_3$ at −78 °C (NMR data is identical to that above). When precooled stock solutions of $LiAlH_4$ and $AlCl_3$ (2.0 molar) were mixed at −78 °C and the perfluorinated alcohol was added within 10 min after mixing, the reaction was quantitative (NMR). **1** was isolated as colorless crystals in 87 % yield by immediate evaporation of the THF solvent, followed by immediate extraction of the remaining white solid with CH_2Cl_2 and subsequent cooling of the concentrated CH_2Cl_2 filtrate to −30 °C. A CH_2Cl_2 solution of **1** decomposes at RT within 12 h to give the ether cleavage product. Solid **1** is stable at RT for weeks.

Cs$^+$[(CF$_3$)$_3$CO]$_2$(Me)Al-F-Al(Me)[OC(CF$_3$)$_3$]$^-$: A 2.0 M solution of $Al(CH_3)_3$ in heptane (1.2 mL, 2.4 mmol) was added dropwise to a cooled solution (−78 °C) of $(CF_3)_3COH$ (1.00 mL, 7.173 mmol) in pentane (10 mL). Slow liberation of methane occurred. After addition of trimethylaluminum (several hours) the flask was allowed to reach 0 °C and than the solvent was evaporated at this temperature. CsF (0.183 g, 1.2 mmol) was added to the residue at 0 °C followed by addition of CH_2Cl_2 (15 mL) at the same temperature. After 2 h stirring at RT a solution above brown solid material resulted that was filtered to give a clear yellow-brownish filtrate. The solid material was discarded. Crystals suitable for X-ray crystallography were obtained from the concentrated CH_2Cl_2 filtrate at −28 °C. Yield: 0.698 g (33 % with respect to nonafluorotertbutanol) as a crystalline compound. ^{13}C NMR (63 MHz, CD_2Cl_2, 25 °C): δ = 121.57 (q, CF_3, $^1J_{CF}$ = 291.1 Hz), 78.80 (sept, $^2J_{CF}$ = 31.1 Hz); ^{27}Al NMR (78 MHz, CD_2Cl_2, 25 °C): δ = 88.7 (s, $\tilde{\nu}_{1/2}$ = 5 kHz); FT-IR(Nujol): $\tilde{\nu}$ = 1247 (s), 1224 (s), 1201 (s), 998 (sh), 968 (vs), 812 (s), 736 (w), 725 (s), 682 (sh), 666 (s), 582 (sh), 440 (s), 370 (s), 356 (m), 340 (w), 310 (s), 292 cm^{-1} (s).

*[Ag(CH$_2$Cl$_2$)$_3$]$^+$[(RO)$_3$Al-F-Al(OR)$_3$]$^-$ [R = C(CF$_3$)$_3$] (**2**):* In a typical procedure $Ag[Al(OR)_4]$ was weighed (9.85 g, 9.16 mmol) into a two bulbed frit plate vessel closed by J. Young valves and dissolved in CH_2Cl_2 (50 mL) to yield a slightly brownish clear solution. Then freshly distilled (!) PCl_3 (0.80 mL; 1.26 g, 9.17 mmol) was added at RT and the mixture wrapped with aluminum foil and stirred for five days at RT. The AgCl precipitated was filtered off and the residue washed several times by back condensing the solvent. Then all volatile materials were removed in the vacuum of an oil pump (weight of the non volatile residue: 8.324 g, expected with the mechanism according to Scheme 2: 8.186 g). Yield: 7.100 g (84 %) spectroscopically pure beige $[Ag(CH_2Cl_2)_x]^+[(RO)_3Al\text{-}F\text{-}Al(OR)_3]^-$ ($x \approx 3$). By further evacuation in the vacuum of a diffusion pump all three coordinated CH_2Cl_2 molecules may be removed within 24 h (NMR). ^{13}C NMR (63 MHz, CD_2Cl_2, 25 °C): δ = 121.0 (q, $^1J_{C,F}$ = 291.0 Hz, CF_3), 79 (m, $C(CF_3)_3$); ^{19}F NMR(288 MHz, CD_2Cl_2, 25 °C): δ = −75.3 (s, CF_3), −184.6 (s, Al-*F*-Al); ^{27}Al NMR (78 MHz, CD_2Cl_2, RT): δ = 33.5 (s, broad); IR (CsI, Nujol): $\tilde{\nu}$ (%) = 1357 (55), 1303 (74), 1277 (86), 1250 (97), 1215 (92), 1181 (61), 976 (100), 864 (33), 760 (22), 727 (87), 665 (29), 641 (37), 571 (32), 538 (43), 453 (40), 376 (27), 330 (18), 319 (26), 296 cm^{-1} (29); elemental analysis calcd (%) for $Ag\text{-}Al_2O_6F_{55}C_{27}H_6Cl_6$ (%): Ag 5.84; found: Ag 5.85.

*[Ag(P$_4$)$_2$]$^+$[(RO)$_3$Al-F-Al(OR)$_3$]$^-$ [R = C(CF$_3$)$_3$] (**3**):* $Ag(CH_2Cl_2)[Al(OR)_4]$ (0.393 g, 0.34 mmol) and P_4 (0.043 g, 0.34 mmol) were weighed into a two bulbed frit plate vessel closed by J. Young valves, dissolved in CH_2Cl_2 (20 mL) and cooled to −78 °C. At this temperature freshly distilled PCl_3 (30 μL, 0.34 mmol) was added through a 50 μL Hamilton syringe with a Teflon canula. The mixture was stirred for 5 days at RT, filtered from the insoluble AgCl and the volatiles of the slightly brownish solution removed until nearly all solvent was removed and an oil had formed. The oil was stored over night at 0 °C when most of the product crystallized in large blocks. The remaining few drops of solution were decanted off at 0 °C and the crystals dried in vacuo to give spectroscopically pure $[Ag(P_4)_2]^+[(RO)_3Al\text{-}F\text{-}Al(OR)_3]^-$ (0.27 g, 86 %). ^{31}P NMR (101 MHz, CD_2Cl_2, 25 °C): δ = −496; ^{31}P NMR (101 MHz, CD_2Cl_2, −80 °C): δ = −487; ^{13}C NMR (63 MHz, CD_2Cl_2, 25 °C): δ = 121.0 (q, $^1J_{C,F}$ = 291.0 Hz, CF_3), 79 (m, $C(CF_3)_3$); ^{27}Al NMR (78 MHz, CD_2Cl_2, RT): δ = 34 (s, broad); Raman: $\tilde{\nu}$ = 804 (w, Al–O), 800 (w, Al–O), 750 (w, Al–O), 600 (vs, P_4-A_g), 472 (s, P_4-B_{2g}), 458 (w, P_4-B_{1g}), 413 (w, P_4-A_g), 381 (sh, P_4-B_{3g}), 373 (s, P_4-A_g), 322 cm^{-1} (w, Al–O).

X-ray Crystallography: The data collections for the X-ray structure determinations were performed on STOE IPDS I and IPDS II diffractometer by using graphite-monochromated $Mo_{K\alpha}$ (0.71073 Å) radiation. Single crystals were mounted in perfluoroether oil on top of a glass fiber and then brought into the cold stream of a low temperature device so that the oil solidified. All calculations were performed on PCs by using the SHELX97 software package. The structures were solved by direct methods and successive interpretation of the difference Fourier maps, followed by least-squares refinement. All non-hydrogen atoms were refined anisotropically. If hydrogen atoms were present in the structures, they were included in the refinement in calculated positions by a riding model using fixed isotropic parameters. Relevant data concerning crystallography, data collection and refinement details are compiled in Table 9.

Table 9. Crystallographic and refinement details of **1**–**3** and $Cs^+[(RO)_2(Me)Al\text{-}F\text{-}Al(Me)(OR)_2]^-$ (CsX).

Compound	**1**	CsX	**2**	**3**
crystal system	orthorhombic	orthorhombic	monoclinic	monoclinic
space group	$Pca2_1$	*Pbca*	*C*2/*c*	*C*2/*c*
a [Å]	17.348(4)	15.663(3)	15.664(3)	19.762(4)
b [Å]	14.992(3)	18.914(4)	13.633(3)	13.059(3)
c [Å]	10.183(2)	24.029(5)	25.565(5)	20.490(4)
α [°]	90	90	90	90
β [°]	90	90	91.73(3)	90.66(3)
γ [°]	90	90	90	90
V [Å^3]	2648.4(9)	7120(10)	5457.2(19)	5287.9(18)
Z	4	8	4	4
ρ_{calcd} [Mg m^{-3}]	2.017	2.195	2.247	2.310
μ [mm^{-1}]	0.293	1.313	0.926	0.983
abs. corr.	–	numerical	numerical	numerical
I_{min}/	–	0.562/	0.649/	0.714/
$I_{max.}$	–	0.876	0.714	0.805
2 θ_{max} [°]	51.62	51.88	51.76	51.94
T [K]	180(2)	150(2)	150(2)	150(2)
refl. colld	18327	40697	18025	20435
refl. unique	5055	6088	5247	5148
refl. obsd (4σ)	4009	4636	3729	4319
R_{int}	0.0650	0.0868	0.0332	0.0559
no. variables	433	560	523	436
GOF	1.014	1.020	1.064	1.043
final *R* (4σ)	0.0625	0.0588	0.0663	0.0349
final *wR*2 (all data)	0.1804	0.1668	0.1873	0.0941

CCDC-211690 (**1**), -211691 ($Cs^+[(RO)_2(Me)Al\text{-}F\text{-}Al(Me)(OR)_2]^-$), -211692 (**2**) and -211693 (**3**) contain the supplementary crystallographic data for this paper. These data can be obtained free of charge via www.ccdc.cam.ac.uk/conts/retrieving.html, or from the Cambridge Crystallographic Data Centre, 12 Union Road, Cambridge CB2 1EZ, UK; fax: (+44)1223–336033; or email: deposit@ccdc.cam.ac.uk.

Computational details: The quantum chemical calculations for the Gibbs energies with inclusion of solvation enthalpies for CH_2Cl_2 at 298 K given in Scheme 2 were done with Turbomole[52] and Gaussian 98.[53] All geometry optimizations with (RI-)BP86/SV(P) and (RI-)MP2/TZVPP,[54,55,56,57] COSMO solvation energy calculations[58] in CH_2Cl_2 and frequency calculations were done with Turbomole. The 28 core electrons of Ag were replaced by a quasi relativistic effective core potential.[57] The thermal and entropic contributions to the Gibbs energy at 298 K were obtained with Gaussian at the PM3-level. All species included in Scheme 2 are true minima with no imaginary frequencies on the respective potential energy surface (BP86/SV(P) quality). For Equations (6a) and (6e) we used MP2/TZVPP calculations as a basis. However, due to the size of the system, we could only use (RI-)BP86/SV(P) for Equations (6b,c,d).

Acknowledgement

We thank Prof. H. Schnöckel for valuable discussions and advice, Dr. H.-J. Himmel, Dipl. Chem. G. Stößer and Dipl. Chem. B. Gärtner for the vibrational spectra. Financial support from the German science foundation DFG and the Fond der Chemischen Industrie as well as donations of chemicals from Merck in Darmstadt are gratefully acknowledged.

[1] Reviews: a) C. Reed, *Acc. Chem. Res.* **1998**, *31*, 133; b) S. H. Strauss, *Chem. Rev.* **1993**, *93*, 927; c) E. Y.-X. Chen, T. J. Marks, *Chem. Rev.* **2000**, *100*, 1391; d) I. Krossing, I. Raabe, *Angew. Chem.* **2004**, *116*, 2116; *Angew. Chem. Int. Ed.* **2004**, *43*, 2066.

[2] a) J. Zhou, S. J. Lancaster, D. A. Walker, S. Beck, M. Thornton-Pett, M. Bochmann, *J. Am. Chem. Soc.* **2001**, *123*, 223; b) R. E. LaPointe, G. R. Roof, K. A. Abboud, J. Klosin, *J. Am. Chem. Soc.* **2000**, *122*, 9560; c) V. C. Williams, G. J. Irvine, W. E. Piers, Z. Li, S. Collins, W. Clegg, M. R. J. Elsegood, T. B. Marder, *Organometallics* **2000**, *19*, 1619; d) E. Y. X. Chen, K. Abboud, *Organometallics* **2000**, *19*, 5541.

[3] a) K. Fujiki, S. Ikeda, H. Kobayashi, A. Mori, A. Nagira, J. Nie, T. Sonoda, Y. Yagupolskii, *Chem. Lett.* **2000**, 66; b) T. J. Barbarich, S. M. Miller, O. P. Anderson, S. H. Strauss, *J. Mol. Catal. A* **1998**, *128(1–3)*, 289.

[4] a) F. Kita, H. Sakata, A. Kawakami, H. Kamizori, T. Sonoda, H. Nagashima, N. V. Pavlenko, Y. Yagzpolskii, *J. Power Sources* **2001**, *97–98*, 581; b) F. Kita, H. Sakata, A. Kawakami, H. Kamizori, T. Sonoda, H. Nagashima, J. Nie, N. V. Pavlenko, Y. Yagzpolskii, *J. Power Sources* **2000**, *90*, 27.

[5] a) R. J. LeSuer, W. E. Geiger, *Angew. Chem.* **2000**, *112*, 254; *Angew. Chem. Int. Ed.* **2000**, *39*, 248; b) F. Barriere, N. Camire, W. E. Geiger, U. T. Mueller-Westerhoff, R. Sanders, *J. Am. Chem. Soc.* **2002**, *124*, 7262; c) N. Camire, A. Nafady, W. E. Geiger, *J. Am. Chem. Soc.* **2002**, *124*, 7260; d) N. Camire, U. T. Mueller-Westerhoff, W. E. Geiger, *J. Organomet. Chem.* **2001**, *637–639*, 823.

[6] a) P. Wasserscheid, W. Keim, *Angew. Chem.* **2000**, *112*, 3926; *Angew. Chem. Int. Ed.* **2000**, *39*, 3772; b) P. Wasserscheid, T. Welton, *Ionic Liquids in Synthesis*, Wiley-VCH, **2003**.

[7] S. Seidel, K. Seppelt, *Science* **2000** *290*, 117.

[8] T. Drews, K. Seppelt, *Angew. Chem.* **1997**, *109*, 264; *Angew. Chem. Int. Ed. Engl.* **1997**, *36*, 273.

[9] C. A. Reed, K.-C. Chan, R. D. Bolskar, L. J. Mueller, *Science* **2000**, *289*, 101.

[10] K. C. Chan, C. A. Reed, D. W. Elliott, L. J. Mueller, F. Tham, L. Lin, J. B. Lambert, *Science* **2002**, *297*, 825.

[11] P. K. Hurlburt, J. J. Rack, J. S. Luck, S. F. Dec, J. D. Webb, O. P. Anderson, S. H. Strauss, *J. Am. Chem. Soc.* **1994**, *116*, 10003.

[12] A. Vij, W. W. Wilson, V. Vij, F. S. Tham, J. A. Sheehy, K. O. Christe, *J. Am. Chem. Soc.* **2001**, *123*, 6308.

[13] B. von Ahsen, M. Berkei, G. Henkel, H. Willner, F. Aubke, *J. Am. Chem. Soc.* **2002**, *124*, 8371.

[14] a) I. Krossing, *J. Am. Chem. Soc.* **2001**, *123*, 4603–4604; b) I. Krossing, L. van Wüllen, *Chem. Eur. J.* **2002**, *8*, 700.

[15] A. Adolf, M. Gonsior, I. Krossing, *J. Am. Chem. Soc.* **2002**, *124*, 7111.

[16] T. S. Cameron, A. Decken, I. Dionne, Min Fang, I. Krossing, J. Passmore, *Chem. Eur. J.* **2002**, *8*, 3386.

[17] A. Reisinger, I. Krossing, *Angew. Chem.* **2003**, *115*, 5903; *Angew. Chem. Int. Ed.* **2003**, *42*, 5725.

[18] a) I. Krossing, *J. Chem. Soc. Dalton Trans.* **2002**, 500; b) I. Krossing, I. Raabe, *Angew. Chem.* **2001**, *113*, 4544; *Angew. Chem. Int. Ed.* **2001**, *40*, 4406.

[19] A. Bihlmeier, I. Krossing, I. Raabe, N. Trapp, *Angew. Chem.* **2003**, *115*, 1569; *Angew. Chem. Int. Ed.* **2003**, *42*, 1531.

[20] I. Krossing, *Chem. Eur. J.* **2001**, *7*, 490.

[21] I. Krossing, H. Brands, R. Feuerhake, S. Koenig, *J. Fluorine Chem.* **2001**, *112*, 83.

[22] a) T. J. Barbarich, S. T. Handy, S. M. Miller, O. P. Anderson, P. A. Grieco, S. H. Strauss, *Organometallics* **1996**, *15*, 3776; b) T. J. Barbarich, S. M. Miller, O. P. Anderson, S. H. Strauss, *J. Mol. Catal. A* **1998**, *128(1–3)*, 289; c) S. M. Ivanova, B. G. Nolan, Y. Kobayashi, S. M. Miller, O. P. Anderson, S. H. Strauss, *Chem. Eur. J.* **2001**, *7*, 503.

[23] C. A. Reed, K.-C. Kim, E. S. Stoyanov, D. Stasko, F. S. Tham, L. J. Mueller, P. D. W. Boyd, *J. Am. Chem. Soc.* **2003**, *125*, 1796.

[24] S. V. Ivanov, J. J. Rockwell, O. G. Polyakov, C. M. Gaudinski, O. P. Anderson, K. A. Solntsev, S. H. Strauss, *J. Am. Chem. Soc.* **1998**, *120*, 4224.

[25] B. T. King, J. Michl, *J. Am. Chem. Soc.* **2000**, *122*, 10255.

[26] $Sb_4F_{21}^-$: T. Drews, K. Seppelt, *Angew. Chem.* **1997**, *109*, 264; *Angew. Chem. Int. Ed. Engl.* **1997**, *36*, 273.

[27] $Sb(OTeF_5)_6^-$: T. S. Cameron, I. Krossing, J. Passmore, *Inorg. Chem.* **2001**, *40*, 2001.

[28] E. Bernhardt, G. Henkel, H. Willner, G. Pawelke, H. Bürger, *Chem. Eur. J.* **2001**, *7*, 4696.

[29] M. Gonsior, I. Krossing, L. Müller, I. Raabe, M. Jansen, L. van Wüllen, *Chem. Eur. J.* **2002**, *8*, 4475.

[30] I. Krossing, R. Feuerhake, unpublished results.

[31] M. Gonsior, I. Krossing, unpublished results.

[32] M. Kaupp, C. Aubauer, G. Engelhardt, T. M. Klapötke, O. Malkina, *J. Chem. Phys.* **1999**, *110*, 3897.

[33] K. B. Dillon, A. W. G. Platt, *Polyhedron* **1983**, *2*, 641.

[34] D. M. Van Seggen, P. K. Hurlburt, O. P. Anderson, S. H. Strauss, *Inorg. Chem.* **1995**, *34*, 3453.

[35] I. Krossing, I. Raabe, *Chem. Eur. J.* **2004**, *10*, in press.

[36] a) D. D. Wagman, W. H. Evans, V. B. Parker, R. H. Schumm, I. Halow, S. M. Bailey, K. L. Churney, R. L. Nuttal, *J. Phys. Chem. Ref. Data* **1982**, *11*, Suppl. 2; b) S. G. Lias, J. E. Bartmess, J. F. Liebman, J. L. Holmes, R. D. Levin, W. G. Mallard, *J. Phys. Chem. Ref. Data* **1988**, *17*, Suppl. 1; c) CRC Handbook of Chemistry and Physics; http://www.nist.gov/chemistry.

[37] J. Weidlein, V. Krieg, *J. Organomet. Chem.* **1968**, *11*, 9.

[38] C. Cui, H. W. Roesky, M. Noltemeyer, M. F. Lappert, H.-G. Schmidt, H. Hao, *Organometallics* **1999**, *18*, 2256.

[39] S. Patrick, T. Pradeep, H. Luo, S. Ma, R. G. Cooks, *J. Am. Soc. Mass Spectrom.* **1998**, *9*, 1158.

[40] L. E. Ramírez-Arizmendi, Y. Q. Yu, H. I. Kenttämaa, *J. Am. Soc. Mass Spectrom.* **1999**, *10*, 379–385.

[41] D. Gudat, *Eur. J. Inorg. Chem.* **1998**, 1087.

[42] Review: D. Gudat, *Coord. Chem. Rev.* **1997**, *163*, 71.

[43] The FIA is the negative reaction enthalpy of the following equation: $A_{(g)} + F^-_{(g)} \xrightarrow{\Delta H = -FIA} AF^-_{(g)}$. The higher the FIA of the Lewis acid A the more reactive it is on thermodynamic grounds.

[44] I. Krossing, N. Trapp, I. Raabe, unpublished results; b) H. P. A. Mercier, M. D. Moran, G. J. Schrobilgen, C. Steinberg, R. J. Suontamo, *J. Am. Chem. Soc.* **2004**, *126*, 5533.

[45] The P–Cl bond in $OPCl_3$ is considerably stronger than in PCl_3 and according to MP2/TZVPP calculations with inclusion of the formation of solid AgCl as well as solvation energies in CH_2Cl_2 the Gibbs energy for the formation of $OPCl_2^+$ and $AgCl_{(s)}$ in CH_2Cl_2 solution is endergonic (COSMO solvation model).

[46] The quantum chemical calculations[52] to obtain the FIA of $Al(OR)_3$ and $2\,Al(OR)_3$ were done with BP86/SV(P). Using this approach we could reproduce the FIAs of BF_3, AlF_3, AsF_5 and SbF_5 as calculated by D. Dixon[47] with a deviation of less than 15 $kJ\,mol^{-1}$ by using the isodesmic reaction $A + OCF_3^- \rightarrow AF^- + OCF_2$ ($A = BF_3$, AlF_3, AsF_5 and SbF_5). See ref. [35] for full details and the isodesmic reaction used to reliably assess the FIA of $2\,Al(OR)_3$.

[47] K. O. Christe, D. A. Dixon, D. McLemore, W. W. Wilson, J. Sheehy, J. A. Bootz, *J. Fluorine Chem.* **2000**, *101*, 151.

[48] I.-C. Hwang, K. Seppelt, *Angew. Chem.* **2001**, *113*, 3803; *Angew. Chem. Int. Ed.* **2001**, *40*, 3690.

[49] a) The LA is the enthalpy of the following reaction: $M(L)_n^- \xrightarrow{\Delta H = LA} M(L)_{n-1} + L^-$ The higher the LA the more stable is the anion against ligand abstraction. b) PD stands for proton decomposition, CuD for copper-decomposition reaction: $M(L)_n^- + H^+ \xrightarrow{\Delta H = PD} M(L)_{n-1} + H\text{-}L$ and $M(L)_n^- + Cu^+ \xrightarrow{\Delta H = CuD} M(L)_{n-1} + Cu\text{-}L$. Since a gaseous anion and a gaseous cation react to give two neutral species, PD and CuD are both exothermic. The less negative PD and CuD values in Table 8 are, the more stable is the WCA against electrophilic attack. The energy of the HOMO of a WCA relates to its resistance towards oxidation. c) The lower the HOMO energy, the more difficult it is to remove an electron and thus to oxidize the WCA. d) The HOMO–LUMO gap in Table 8 can be associated with the resistance of an anion towards reduction and the larger the gap, the more stable is the anion with respect to reduction. Very small gap's such as those of $[Sb_4F_{21}]^-$ or $[As(OTeF_5)_6]^-$ are an indication of the potentially oxidizing character of these anions. e) As a measure for the coordinating ability of an anion the partial charges of the most negatively charged atom ($q_{neg.}$) as well as the most negatively charged surface atom ($q_{surf.}$) are collected in Table 8. It is clear that low charges are an indication for low coordination ability. However, steric effects may also be of importance and the most basic atoms may be hidden in the center of a large WCA and are, therefore, *not* available for coordination. In this case the charge of the most basic accessible surface atoms $q_{surf.}$ appears to be a better measure.

[50] a) D. V. Deubel, *J. Am. Chem. Soc.* **2002**, *124*, 12312; b) H.-C. Tai, C. Lim, I. Krossing, M. Seth, D. V. Deubel, *Organometallics* **2004**, *23*, 2343.

[51] a) M. Di Vaira, P. Stoppioni, M. Peruzzini, *J. Chem. Soc. Dalton Trans.* **1990**, 109; b) M. Di Vaira, M. P. Ehses, M. Peruzzini, P. Stoppioni, *Polyhedron* **1999**, *18*, 2331.

[52] Turbomole, Version 5: a) R. Ahlrichs, M. Bär, M. Häser, H. Horn, C. Kölmel, *Chem. Phys. Lett.* **1989**, *162*, 165; b) M. v. Arnim, R. Ahlrichs, *J. Chem. Phys.* **1999**, *111*, 9183; c) O. Treutler, R. Ahlrichs, *J. Chem. Phys.* **1995**, *102*, 346; current version: http://www.chemie.uni-karlsruhe.de/PC/TheoChem

[53] Gaussian 98, Revision A.3, Gaussian, Inc., Pittsburgh PA, **1998**.

[54] a) K. Eichkorn, F. Weigend, M. Häser, R. Ahlrichs, *Theor. Chim. Acta* **1997**, *97*, 331; b) K. Eichkorn, O. Treutler, H. Ohm, M. Häser, R. Ahlrichs, *Chem. Phys. Lett.* **1995**, *242*, 652.

[55] a) J. P. Perdew, *Phys. Rev. B* **1986**, *33*, 8822; b) A. D. Becke, *Phys. Rev. A* **1988**, *38*, 3098; c) S. H. Vosko, L. Wilk, M. Nusair, *Can. J. Phys.* **1980**, *58*, 1200.

[56] a) A. Schäfer, H. Horn, R. Ahlrichs, *J. Chem. Phys.* **1992**, *97*, 2571; b) A. Schäfer, C. Huber, R. Ahlrichs, *J. Chem. Phys.* **1994**, *100*, 5829.

[57] D. Andrae, U. Haeussermann, M. Dolg, H. Stoll, H. Preuss, *Theor. Chim. Acta* **1990**, *77*, 123.

[58] A. Klamt, G. Schürmann, *J. Chem. Soc. Perkin Trans. 2* **1993**, 799.

Received: January 30, 2004
Published online: August 30, 2004

